Acta Astronautica 105 (2014) 95–100

Contents lists available at ScienceDirect

Acta Astronautica

journal homepage: www.elsevier.com/locate/actaastro

Experimental investigation of fuel regression rate in a HTPB based lab-scale hybrid rocket motor ☆

Xintian Li, Hui Tian *, Nanjia Yu, Guobiao Cai

School of Astronautics, Beihang University, Beijing 100191, China

ARTICLE INFO

Article history:
Received 25 March 2014
Received in revised form
26 July 2014
Accepted 29 August 2014
Available online 8 September 2014

Keywords:
Fuel regression rate
Hydrogen peroxide
Metal additive
Hybrid rocket motor

ABSTRACT

The fuel regression rate is an important parameter in the design process of the hybrid rocket motor. Additives in the solid fuel may have influences on the fuel regression rate, which will affect the internal ballistics of the motor. A series of firing experiments have been conducted on lab-scale hybrid rocket motors with 98% hydrogen peroxide (H_2O_2) oxidizer and hydroxyl terminated polybutadiene (HTPB) based fuels in this paper. An innovative fuel regression rate analysis method is established to diminish the errors caused by start and tailing stages in a short time firing test. The effects of the metal Mg, Al, aromatic hydrocarbon anthracene ($C_{14}H_{10}$), and carbon black (C) on the fuel regression rate are investigated. The fuel regression rate formulas of different fuel components are fitted according to the experiment data. The results indicate that the influence of $C_{14}H_{10}$ on the fuel regression rate of HTPB is not evident. However, the metal additives in the HTPB fuel can increase the fuel regression rate significantly.

1. Introduction

Hybrid rocket motor uses liquid oxidizer and solid fuel as propellants. It has many advantages, such as safety, low cost, throttling, and shutdown characteristics, compared with a solid or liquid rocket propulsion system. It can be used in the applications of sounding rockets, target drones, large launch boosters, and suborbital manned spaceships [1–5]. The fuel regression rate is a key parameter which will directly affect the internal ballistics of the motor. It is affected by the propellant combinations, oxidizer mass flow rates, fuel types, and fuel components [6–9].

The working process of the hybrid rocket motor is diffusion controlled. Therefore, the fuel regression rate is much lower than that of the solid rocket motor. Analytical studies of hybrid rocket combustion by Marxman et al. relied on boundary layer assumptions to determine the heat flux to the fuel surface which characterizes the fuel regression rate. In Marxman's analysis, the fuel regression rate depends primarily on the mass flow rate of the oxidizer, which is given as $r=aG_o^n$. The coefficients a and n are constants for a certain propellant combination and motor configuration. Most of the experimental researches of the fuel regression rate were based on this formula.

George et al. conducted experimental investigation on the methods of enhancing the fuel regression rate in hydroxyl terminated polybutadiene (HTPB) fuel and gaseous oxygen hybrid rocket motor [8]. The addition of ammonium perchlorate (AP) and/or aluminum in the fuel and the reduction of grain port diameter enhanced the regression rate. Einav established a laboratory-scale setup for hot-fire testing of a modular hybrid rocket motor [10]. Experimental evaluation of the effect of several additives on the fuel regression rates of HTPB-based fuels

☆ This paper was presented during the 64th IAC in Beijing.

* Corresponding author. Tel.: +86 10 82338117; fax: +86 10 82338798.
E-mail addresses: lxtsul@gmail.com, lxt@sa.buaa.edu.cn (X. Li), tianhui@buaa.edu.cn (H. Tian), ynj@buaa.edu.cn (N. Yu), cgb@buaa.edu.cn (G. Cai).

http://dx.doi.org/10.1016/j.actaastro.2014.08.028
0094-5765/

was presented. Five fuel formulas with various additive content of fine AP, polystyrene (PS), and catalyst were tested. A significant enhancement of the regression rate was obtained with the addition of both fine AP and large particles of PS, but combustion extinguishment was not possible with high AP content. Risha et al. conducted an experimental investigation to determine the relation propulsive performance of various HTPB-based solid-fuel formulations containing nano-sized energetic metal particles [11]. These particles included Alex particles, WARP-1 aluminum particles, and B_4C. The addition of energetic powders showed an increment of up to 50% in mass burning rate compared to the pure HTPB fuel.

Plenty of experiments on the fuel regression rate were conducted in the past. However, few works focused on the fuel regression rate analysis method, which may lead to analysis errors under some circumstances. In addition, experiments of hybrid rocket motor with 98% high concentration hydrogen peroxide (H_2O_2) are less reported. The purpose of this paper is to establish an innovative fuel regression rate analysis method to diminish the errors caused by the start and tailing stages in short-time tests. With this method, the fuel regression rates of the hybrid rocket motor with 98% high concentration H_2O_2 and HTPB based fuels are obtained. The additives in the fuel include metal Mg, Al, aromatic hydrocarbon anthracene ($C_{14}H_{10}$), and carbon black (C). A series of tests are performed to get the fuel regression rates of these fuel components under various oxidizer mass flow rates. The duration of each firing test is 5 s. With the experimental data, the fuel regression rate formulas are fitted and compared with each other.

2. Experimental setup

2.1. Motor configuration

The experimental tests are carried out on a modular lab-scale hybrid rocket motor with the fuel outer diameter of 100 mm, which is called a Φ100 hybrid rocket motor. The motor consists of a head oxidizer chamber, an injector panel, an igniter, a forward vaporization chamber, a solid fuel, an aft mixing chamber, and a conical nozzle. Fig. 1 shows the experimental hybrid rocket motor configuration. Fig. 2 shows the photograph of the motor components. Table 1 presents the main parameters of the Φ100 hybrid rocket motor.

The configuration of the motor is mainly made of structural steel. The nozzle is made of copper infiltrated tungsten material for its high heat conduction coefficient. For the both forward vaporization chamber and aft mixing chamber, high silica fiber thermal isolation layers are settled in them to prevent the heat from conducting to the metal structure.

High concentration H_2O_2 can provide more energy for the combustion, which will increase the specific impulse and motor performances. However, the adiabatic decomposition temperature of 98% H_2O_2 is about 1224 K. It will increase the cost and difficulty to develop a catalytic bed. Therefore, an annular igniter is designed as the ignition system. A cuboid solid rocket motor fuel grain is settled in the annular chamber. There are 12 radial holes inside of the igniter. The combustion flames eject from the holes to the central port of the motor, which provide energy for the decomposition of H_2O_2. The stable working time of the igniter can last about 3 s.

The fuel of the hybrid rocket motor is HTPB based. The additives in the fuel include metal Mg, Al, $C_{14}H_{10}$, and C. Three kinds of fuels are investigated in this paper, which are shown in Table 2.

2.2. Oxidizer delivery system

The pressure feeding scheme is used for the oxidizer delivery system. The high pressure nitrogen gas source can provide a steady pressure for the oxidizer tank.

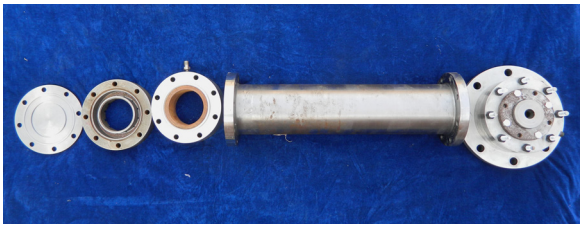

Fig. 2. Photograph of the hybrid rocket motor components.

Table 1
Parameters of the Φ100 hybrid rocket motor.

Parameter	Value
Fuel grain outer diameter (mm)	100
Fuel grain inner diameter (mm)	50
Fuel grain length (mm)	500
Forward vaporization chamber length (mm)	40
Aft mixing chamber length (mm)	50
Nozzle throat diameter (mm)	18
Nozzle expansion area ratio	3

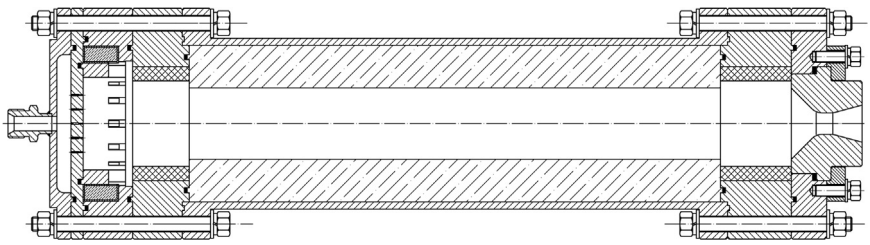

Fig. 1. Experimental hybrid rocket motor configuration.

The oxidizer mass flow rate is controlled by the cavitating venturi tube. If the throat of the venturi tube is in the cavitating condition, the oxidizer mass flow rate is only controlled by the inlet pressure

$$\dot{m}_o = \mu A\sqrt{2\rho_o(p_1 - p_{sat})} \quad (1)$$

where μ is the discharge coefficient, which can be acquired by the water flow calibration experiment. A is the area of the venturi tube throat, ρ_o is the density of H_2O_2, p_1 is the inlet pressure of the venturi tube, and p_{sat} is the saturation pressure of H_2O_2.

2.3. Measurement and control system

The measurement system adopts National Instruments devices to acquire the experimental data during the test, including pressures at different locations and the motor thrust. The PXI bus is used in the measurement system. The system can provide more than 200 channels for the test. The sampling rate can reach 62.5 k samples per second per channel. The cabinets of the measurement system are shown in Fig. 3. The main function of the cabinet is to transfer the standard 4–20 mA electric current signal exported by the measurement sensor to 1–5 V voltage signal. Then the signal will be received by the measurement card and acquired by the computer. Several pressure sensors are settled in the delivery system and the combustion chamber. The measurement range of the sensor is 6 MPa or 10 MPa, and the percentage error is 0.2%.

The Programmable Logic Controller (PLC) is selected to control the igniter and valves in tests. The output of the control system can be controlled by both control panel hardware and control system program. Fig. 4 shows the photograph of the control panel hardware. The igniter and valves are driven by 24 V and 27 V direct current, respectively. In the experiment, the output signals should be arranged in a certain time sequence, which is set in the control system program on the computer.

The igniter provides energy for the decomposition of H_2O_2 and pyrolysis of the solid fuel. In the time sequence of the test, the igniter starts working 1 s before the opening of the oxidizer feeding valve. Each test lasts for 5 s. At the end of the test, purging nitrogen gas is used to terminate the combustion of the motor. Table 3 shows the time sequence of the firing test.

Table 2
Solid fuel formulas of the hybrid rocket motor.

Fuel ID	Fuel formula	ρ (g/cm^3)
A	80% HTPB+20% Al	1.066
B	60% HTPB+20% $C_{14}H_{10}$+20% Al	1.110
C	60% HTPB+28% Al+10% Mg+2% C	1.192

Table 3
Time sequence of the firing test.

No.	Time(s)	Name	Action
1	0.0	Measurement trigger	On
2	1.0	Igniter firing signal	On
3	1.2	Igniter firing signal	Off
4	2.0	Oxidizer feeding valve	On
5	7.0	Oxidizer feeding valve	Off
6	7.0	Purging nitrogen gas valve	On
7	17.0	Purging nitrogen gas valve	Off
8	18.0	Measurement trigger	Off

Fig. 3. Cabinets of the measurement system.

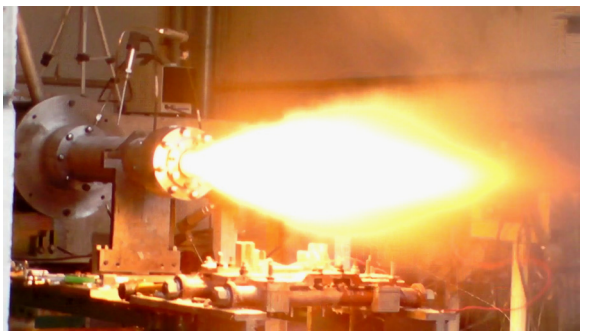

Fig. 5. Photograph of the hybrid rocket motor firing test.

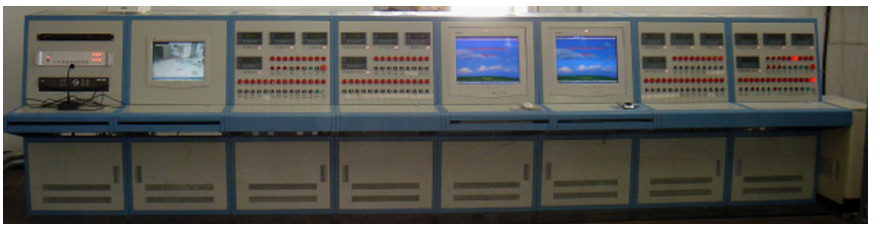

Fig. 4. Photograph of the control panel hardware.

3. Results and discussion

3.1. Experimental results

Fifteen firing tests are performed all together with five tests of each kind of fuel formula. The oxidizer mass flow rate in all tests is about 350 g/s. The igniter scheme is demonstrated to be effective and all of the tests are successful. Fig. 5 shows the photograph of a firing test. Fig. 6 shows the solid fuel of the hybrid rocket motor before and after the test.

Fig. 7 shows the classical experiment curves of a test. The working process of the firing is steady. Oscillation phenomenon is not observed in the test. The pressure peak at the time 1 s is caused by the igniter. The oxidizer valve is open at the time of 2 s. The oxidizer feeding time of the tube after oxidizer valve and head oxidizer chamber takes about 300 ms before the pressure and thrust begin to increase. There are two pressure peaks in the both start and tailing of the test. The peak at the combustion chamber pressure built stage is due to the working of the igniter, which adds additional energy to the flow domain. The pressure peak at the tailing is caused by the high pressure purging nitrogen gas, which blows the residual H_2O_2 in the head oxidizer chamber into the combustion chamber. The transient high oxidizer mass flow rate leads to the pressure peak at the tailing. These two stages may affect the accuracy of the fuel regression rate analysis.

3.2. Fuel regression rate analysis method

The working time of the test is not very long; thus the average fuel regression rate approach is assumed to be feasible. However, the traditional fuel regression rate analysis method assumes that the fuel regression rate in the entire working time is uniform. The errors caused by the start and tailing stages are neglected. In fact, the fuel regression rates in these stages are not identical with that of the steady combustion stage. Therefore, a fuel regression rate analysis method should be proposed to diminish these errors.

For the convenience of the later discussion, we make two definitions at first.

The working time t_a: it starts from the time t_{ai} when the combustion chamber pressure increases to 10% of the steady value, and it ends at the time t_{at} when the combustion chamber pressure drops to 10% of the steady value after the motor is shut off.

The stable working time t_s: it starts from the time t_{si} when the combustion chamber pressure increases to 90% of the steady value, and it ends at the time t_{st} when the combustion chamber pressure drops to 90% of the steady value after the oxidizer valve is closed. The definitions of these time points and durations are shown in Fig. 7.

The consumption of the fuel in the whole working time m_{fa} can be measured by weighting the motor before and after the test. However, the fuel is not consumed uniformly in the working time. Therefore, the average fuel regression rate in the entire working time is different with that of the stable working time.

The equilibrium combustion chamber pressure can be calculated as follows:

$$p_c = \frac{c^*\dot{m}}{A_t} = \frac{c^*(\dot{m}_o + \dot{m}_f)}{A_t} = \frac{c^*\dot{m}_f}{A_t}(r_{of} + 1) \tag{2}$$

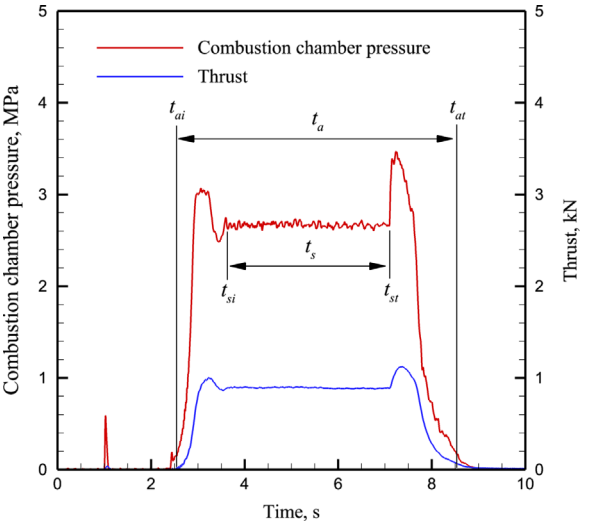

Fig. 7. Classical experiment curves of a test.

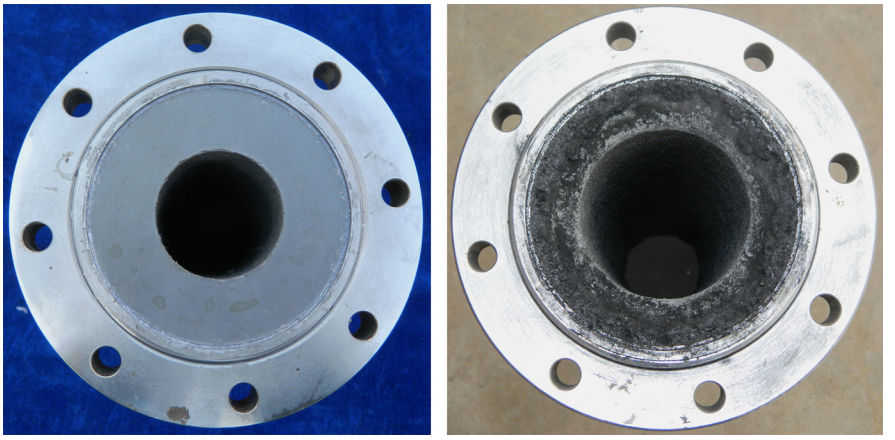

Fig. 6. Solid fuel of the motor before and after a test.

where c^* is the characteristic velocity and r_{of} is the oxidizer to fuel ratio.

The combustion chamber pressure p_c is related to the total mass flow rate $\dot{m}$. The nozzle throat area A_t is almost a constant in the short time firing test. Without considering the changes of the characteristic velocity c^* and the oxidizer to fuel ratio r_{of} in the working process of the motor, we have

$$p_c \propto \dot{m}_f \tag{3}$$

Although c^* and r_{of} are not constants in the working time, Eq. (3) seems to be more reasonable than the whole working time average regression rate method. In the both pressure build up and tailing off stages, the fuel regression rate is lower, which matches well with the lower combustion chamber pressure of the two stages. Therefore, the above assumption is considered to be feasible.

The value of the combustion chamber pressure can reflect the consumption rate of the fuel approximately. Assuming that the consumption rate of the fuel is proportional to the combustion chamber pressure, the consumption of the fuel in the stable working time m_{fs} can be expressed as follows:

$$m_{fs} = m_{fa}\frac{\int_{t_{si}}^{t_{st}} p_c \mathrm{d}t}{\int_{t_{ai}}^{t_{at}} p_c \mathrm{d}t} \tag{4}$$

Correspondingly, the masses of the fuel consumed in the start and tailing stages can be calculated similarly.

$$m_{fsi} = m_{fa}\frac{\int_{t_{ai}}^{t_{si}} p_c \mathrm{d}t}{\int_{t_{ai}}^{t_{at}} p_c \mathrm{d}t} \tag{5}$$

$$m_{fst} = m_{fa}\frac{\int_{t_{st}}^{t_{at}} p_c \mathrm{d}t}{\int_{t_{ai}}^{t_{at}} p_c \mathrm{d}t} \tag{6}$$

Obviously

$$m_{fa} = m_{fsi} + m_{fs} + m_{fst} \tag{7}$$

According to the fuel geometry parameters, we have

$$r_{at} = \sqrt{r_{ai}^2 + \frac{m_{fa}}{\pi \rho_f L_f}} \tag{8}$$

$$r_{si} = \sqrt{r_{ai}^2 + \frac{m_{fsi}}{\pi \rho_f L_f}} \tag{9}$$

$$r_{st} = \sqrt{r_{si}^2 + \frac{m_{fs}}{\pi \rho_f L_f}} \tag{10}$$

Then we can get the average fuel regression rate $\dot{r}$ in the stable working time

$$\dot{r} = \frac{r_{st} - r_{si}}{t_s} \tag{11}$$

The oxidizer mass flow rate $\dot{m}_o$ can be obtained from Eq. (1), and then the average oxidizer mass flux G_o in the stable working time can be calculated as follows:

$$G_o = \frac{\int_{r_{si}}^{r_{st}} (\dot{m}_o/\pi r^2)\mathrm{d}r}{r_{st} - r_{si}} = \frac{\dot{m}_o}{\pi r_{si} r_{st}} \tag{12}$$

The fuel regression rate is usually assumed to be governed by the oxidizer mass flux, which is widely used in experimental research for its simple expression [12–14]. The fuel regression rate law can be expressed as follows:

$$\dot{r} = aG_o^n \tag{13}$$

Then, the linearized equation can be expressed by the logarithmic format

$$\ln \dot{r} = \ln a + n \ln G_o \tag{14}$$

3.3. Comparison of fuel regression rates

For each kind of fuel formula, five firing tests are conducted. Although the oxidizer mass flow rate is constant, the fuel port area increases with the increasing working time. Therefore, we can get the average fuel regression rates under different oxidizer mass fluxes. According to Eq. (14), the constants a and n can be obtained by the least square fitting method. Fig. 8 shows the experimental data and fitting curves of the fuel regression rates of different fuel formulas. The correlation between the fuel regression rate points and the fitting curve of each fuel shows to be well. Table 4 presents the fuel regression rate formulas fitted by the experimental data.

As shown in the figure and the table, the regression rate of the fuel A and fuel B are similar under the same oxidizer mass flux. The metal Al proportions of the two fuel

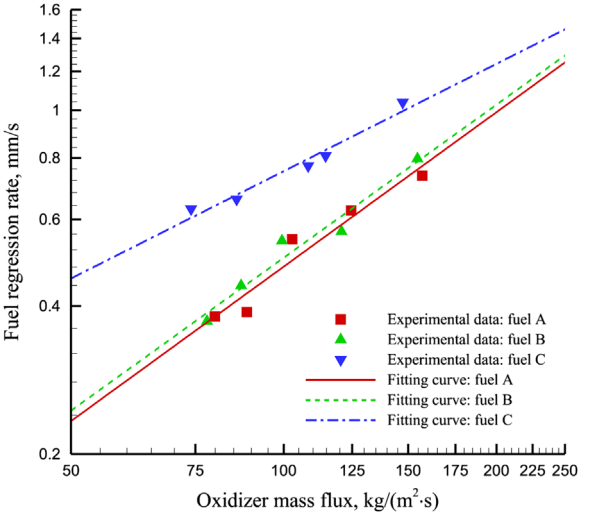

Fig. 8. Fuel regression rate data and fitting curves.

Table 4
Regression rate formulas of different fuel components.

Fuel ID	Fuel regression rate formula
A	$r = 3.9388 \times 10^{-6} G_o^{1.0433}$
B	$r = 4.2938 \times 10^{-6} G_o^{1.0336}$
C	$r = 2.6676 \times 10^{-5} G_o^{0.72493}$

formulas are identical, yet there is 20% $C_{14}H_{10}$ instead of HTPB in the fuel B. This suggests that $C_{14}H_{10}$ does not have obvious influence on the fuel regression rate of HTPB based fuel. Because $C_{14}H_{10}$ and HTPB are both hydrocarbons, the physical property and the thermal conductivity coefficient of them are similar. Therefore, the fuel regression rate characteristics of them are alike. However, the addition of $C_{14}H_{10}$ can increase the density of the fuel, which may improve the density specific impulse of the motor.

The regression rate of the fuel C is much larger than that of the fuel A and fuel B under same oxidizer mass flux. The metal additive of the fuel C is higher than those of the fuel A and B. It indicates that the addition of metal Mg and Al will increase the fuel regression rate. This result is in accordance with the research in the reference [11]. The metal powder in the fuel may increase the radiative heat flux and improve the heat transfer coefficient of the fuel. Therefore, the regression rate of the fuel A is higher. In addition, the metal can improve the density of the fuel and density specific impulse of the motor. However, large proportion of the metal powder in the fuel may lead to the two-phase flow loss in the nozzle. This effect should be considered in the future studies.

4. Conclusion

This paper presents the experimental studies of the fuel regression rates of lab-scale hybrid rocket motors with 98% H_2O_2 oxidizer and HTPB based fuels. Fifteen firing tests are successfully performed on the Φ100 mm modular hybrid rocket motor. The fuel regression rates of three kinds of fuel formulas with the additives Mg, Al, $C_{14}H_{10}$, and C are investigated. An average fuel regression rate analysis method is put forward for short time firing test to diminish the errors caused by the start and tailing stages. With this analysis method, the regression rates of each fuel formula under different oxidizer mass fluxes are acquired. Then the fuel regression rate formulas are fitted, and the correlation between the fuel regression rate points and the fitting curve of each fuel shows to be well. The results indicate that the influence of $C_{14}H_{10}$ to the fuel regression rate of HTPB is not evident. The addition of the metal powder Mg and Al can increase the fuel regression rate obviously. In addition, the addition of $C_{14}H_{10}$, Mg, and Al can increase the density of the fuel, which is a benefit for increase of the density specific impulse of the hybrid rocket motor.

References

[1] M.J. Chiaverini, K.K. Kuo, Fundamentals of Hybrid Rocket Combustion and Propulsion, 218, American Institute of Aeronautics and Astronautics, Inc., Virginia, 2006.
[2] J. Tsohas, B. Appel, A. Rettenmaier, M. Walker, S.D. Heister, Development and launch of the Purdue hybrid rocket technology demonstrator, in: Proceedings of the 45th AIAA/ASME/SAE/ASEE Joint Propulsion Conference & Exhibit, Denver, Colorado, 2–5 August 2009, AIAA Paper 2009-4842.
[3] F.W. Taylor, R. Howard, Dream chaser for space transportation: tourism, NASA and military integrated on an Atlas V, in: Proceedings of the AIAA SPACE 2008 Conference & Exposition, San Diego, California, September 2008, AIAA Paper 2008-7837.
[4] B. Evans, E. Boyer, K.K. Kuo, G. Risha, M. Chiaverini, Hybrid rocket investigations at Penn State University's high pressure combustion laboratory: overview and recent results, in: Proceedings of the 45th AIAA/ASME/SAE/ASEE Joint Propulsion Conference & Exhibit, Denver, Colorado, 2–5 August 2009, AIAA Paper 2009-5349.
[5] G. Story, T. Zoladz, J. Arves, D. Kearney, Hybrid propulsion demonstration program 250 K hybrid motor, in: Proceedings of the 39th AIAA/ASME/SAE/ASEE Joint Propulsion Conference and Exhibit, Huntsville, Alabama, 2003, AIAA Paper 2003-5198.
[6] G.A. Marxman, M. Gilbert, Turbulent boundary layer combustion in the hybrid rocket, Symp. (Int.) Combust. 9 (1963) 371–383.
[7] M.J. Chiaverini, K.K. Kuo, A. Peretz, G.C. Harting, Regression rate and heat transfer correlations for HTPB/GOX combustion in a hybrid rocket motor, 1998, AIAA Paper 98-3185.
[8] P. George, S. Krishnan, P.M. Varkey, M. Ravindran, L. Ramachandran, Fuel regression rate in hydroxyl-terminated-polybutadiene/gaseous-oxygen hybrid rocket motors, J. Propuls. Power 17 (1) (2001) 35–42.
[9] X. Li, H. Tian, G. Cai, Numerical analysis of fuel regression rate distribution characteristics in hybrid rocket motors with different fuel types, Sci. China Technol. Sci. 56 (7) (2013) 1807–1817.
[10] O. Einav, A. Peretz, B. Hashmonay, A. Birnholz, Z. Sobe, Development of a lab-scale system for hybrid rocket motor testing, in: Proceedings of the 45th AIAA/ASME/SAE/ASEE Joint Propulsion Conference & Exhibit, Denver, Colorado, 2–5 August 2009, AIAA 2009-4888.
[11] G.A. Risha, A. Ulas, E. Boyer, S. Kumar, K.K. Kuo, Combustion of HTPB-based solid fuels containing nano-sized energetic powder in a hybrid rocket motor, in: Proceedings of the 37th AIAA/ASME/SAE/ASEE Joint Propulsion Conference and Exhibit, Salt Lake City, Utah, 2001, AIAA Paper 2001-3535.
[12] G.A. Marxman, C.E. Wooldridge, R.J. Muzzy, Fundamentals of hybrid boundary layer combustion, in: Proceedings of the Heterogeneous Combustion Conference, Palm Beach, Florida, 11–13 December 1963, AIAA Paper 1963-0505.
[13] E. Farbar, J. Louwers, T. Kaya, Investigation of metallized and nonmetallized hydroxyl terminated polybutadiene/hydrogen peroxide hybrid rockets, J. Propuls. Power 23 (2) (2007) 476–486.
[14] A. Lewin, J. Dennis, B. Conley, D. Suzuki, Experimental determination of performance parameters for a polybutadiene/oxygen hybrid rocket, in: Proceedings of the AIAA/SAE/ASME/ASEE 28th Joint Propulsion Conference and Exhibit, Nashville, TN, 6–8 July 1992, AIAA Paper 92-3590.